INFECTION AND IMMUNITY, July 2011, p. 2619–2631 Vol. 79, No. 7
0019-9567/11/$12.00 doi:10.1128/IAI.05152-11

Transcriptome of *Proteus mirabilis* in the Murine Urinary Tract: Virulence and Nitrogen Assimilation Gene Expression▽†

Melanie M. Pearson,‡ Alejandra Yep, Sara N. Smith, and Harry L. T. Mobley*

Department of Microbiology and Immunology, University of Michigan Medical School, Ann Arbor, Michigan 48109

Received 20 December 2010/Returned for modification 8 February 2011/Accepted 8 April 2011

The enteric bacterium *Proteus mirabilis* is a common cause of complicated urinary tract infections. In this study, microarrays were used to analyze *P. mirabilis* gene expression *in vivo* from experimentally infected mice. Urine was collected at 1, 3, and 7 days postinfection, and RNA was isolated from bacteria in the urine for transcriptional analysis. Across nine microarrays, 471 genes were upregulated and 82 were downregulated *in vivo* compared to *in vitro* broth culture. Genes upregulated *in vivo* encoded mannose-resistant *Proteus*-like (MR/P) fimbriae, urease, iron uptake systems, amino acid and peptide transporters, pyruvate metabolism enzymes, and a portion of the tricarboxylic acid (TCA) cycle enzymes. Flagella were downregulated. Ammonia assimilation gene *glnA* (glutamine synthetase) was repressed *in vivo*, while *gdhA* (glutamate dehydrogenase) was upregulated *in vivo*. Contrary to our expectations, ammonia availability due to urease activity in *P. mirabilis* did not drive this gene expression. A *gdhA* mutant was growth deficient in minimal medium with citrate as the sole carbon source, and loss of *gdhA* resulted in a significant fitness defect in the mouse model of urinary tract infection. Unlike *Escherichia coli*, which represses *gdhA* and upregulates *glnA in vivo* and cannot utilize citrate, the data suggest that *P. mirabilis* uses glutamate dehydrogenase to monitor carbon-nitrogen balance, and this ability contributes to the pathogenic potential of *P. mirabilis* in the urinary tract.

The urinary tract is a common site of infection (for a recent review see reference 57). Recent strides have been made in understanding the pathogenesis of uropathogenic *Escherichia coli* (UPEC), the most common cause of urinary tract infection (UTI) in otherwise healthy individuals. There are now studies defining UPEC transcription during experimental UTI in mice (74), asymptomatic bacteriuria in humans (70), and human UTI (22). However, far less is known about bacterial agents of complicated UTI, which occurs in catheterized patients or patients with structural or functional abnormalities of the urinary tract and is frequently polymicrobial (28). UTI is the most common type of nosocomial infection, causing an estimated 424,000 cases and 13,000 deaths in U.S. hospitals in 2002 (34). *Proteus mirabilis* is one of the major causes of complicated UTI (81, 82) and is associated with particularly severe disease due to its ability to cause nephrolithiasis (kidney stones) and block urinary catheters (32, 41, 54).

P. mirabilis, a member of the *Enterobacteriaceae*, is well known for its ability to swarm across solid surfaces (55, 64). Urease, which mediates the hydrolysis of urea into ammonia and carbon dioxide, is perhaps the most potent virulence factor of *P. mirabilis*. Urease activity increases the pH of urine, leading to the precipitation of minerals and stone formation (53); it is required for *P. mirabilis* virulence during experimental UTI (33). *P. mirabilis* carries genes that encode 17 putative fimbrial operons (65), 5 of which have been named: MR/P (mannose-resistant *Proteus*-like) (9, 60), PMF (*P. mirabilis* fimbriae) (50), UCA (uroepithelial cell adhesin) (15, 85), PMP (*P. mirabilis* P-like pili) (11), and ATF (ambient-temperature fimbria) (47, 48). Two of these, MR/P (8) and PMF (49, 86), have been shown to play a role in virulence during experimental UTI and have been the focus of vaccine efforts (39, 66). Other known virulence factors for this organism include flagella (3, 51), toxins (HpmAB) (77, 80), proteases (Zap [83] and Lon [13]), autotransporters (Pta [2] and AipA and TaaP [1]), iron (27, 42) and zinc (59) uptake, and capsule (16). Signature-tagged mutagenesis studies have also highlighted the importance of central metabolism in the disease process (12, 26). Recent microarray studies examined total gene transcription during swarming (64) and iron restriction (27).

In this article, we investigate for the first time the transcriptome of *P. mirabilis* during infection, using a mouse model of ascending UTI. This is also the first study that investigates global transcription over time during UTI. The results have many parallels with UPEC gene expression during murine and human UTI, but also some important differences. Probing the distinctions in *P. mirabilis* and UPEC gene expression led to the discovery of an unexpected novel role for glutamate dehydrogenase (GDH) in *P. mirabilis* metabolism.

MATERIALS AND METHODS

Bacterial strains and culture conditions. *P. mirabilis* HI4320, isolated from the urine of an elderly, long-term-catheterized woman, has been previously described (54), sequenced, and annotated (65). *E. coli* CFT073 was isolated from the blood and urine of a patient with acute pyelonephritis (52) and has also been sequenced and annotated (84). The *P. mirabilis ureC* mutant has been previously reported (33). *E. coli* DH5α was used as the host for cloning mutational constructs. Bacteria were routinely cultured at 37°C with aeration in LB broth (10 g/liter tryptone, 5 g/liter yeast extract, 0.5 g/liter NaCl) or on LB solidified with 1.5% agar. The urease mutant was also cultured in filter-sterilized, pooled human urine from healthy adult volunteers. For studies on the effect of carbon

* Corresponding author. Mailing address: 5641 Medical Science Bldg. II, 1150 W. Med. Ctr. Dr., Ann Arbor, MI 48109-0620. Phone: (734) 764-1466. Fax: (734) 763-7163. E-mail: hmobley@umich.edu.

‡ Present address: Department of Microbiology, New York University School of Medicine, New York, NY 10016.

† Supplemental material for this article may be found at http://iai.asm.org/.

▽ Published ahead of print on 19 April 2011.

source on *P. mirabilis* growth and gene transcription, minimal A medium (10) was utilized with 1% glucose, glycerol, citrate, or acetate as the carbon source.

Mouse model of ascending UTI. To investigate *in vivo* gene transcription by *P. mirabilis* during UTI, 30 female CBA/J mice were transurethrally inoculated with approximately 1×10^7 CFU of *P. mirabilis* HI4320, using a modification (32) of a previously published method (23). Briefly, an overnight culture of wild-type *P. mirabilis* HI4230 was adjusted to an estimated density of 2×10^8 CFU/ml (optical density at 600 nm [OD_{600}] of 0.2). Six- to 8-week-old female CBA/J mice were inoculated transurethrally with 50 μl of the suspension (i.e., 1×10^7 CFU) via a sterile polyethylene catheter, using an infusion pump (Harvard Apparatus). At 1, 3, and 7 days postinfection, urine was collected from mice directly into 14-ml polypropylene round-bottom tubes (Falcon, Becton-Dickinson) containing RNA Protect (Qiagen). At least 4 ml urine was collected per time point per experiment. Two milliliters of RNA Protect was used per ml of urine collected. The RNA-stabilized urine was placed on ice for at least 1 h, after which the fluid was separated from a crystalline precipitate that had formed (74). The fluid was centrifuged (10 min, 7,000 × *g*, 4°C), and the bacterial pellet was stored at −20°C before RNA extraction. The University of Michigan University Committee on Use and Care of Animals approved all mouse protocols.

RNA extraction and microarray analysis. RNA was isolated with the RNeasy minikit (Qiagen). One column was used per ml of urine collected. RNA was treated with DNase (Ambion) and concentrated with an RNeasy MinElute column (Qiagen). The entire RNA sample (2 to 4 μg) was converted to cDNA and labeled with Cy5 CyDye (GE Healthcare) as previously reported (64). As a comparison condition, RNA was extracted from a mid-logarithmic-phase (OD_{600} of 1.0) *P. mirabilis* HI4320 LB broth culture, converted to cDNA, and labeled with Cy3. The *in vivo* and *in vitro* cDNA samples were hybridized with a *P. mirabilis* HI4320-specific microarray as previously described (64). Slides were scanned with a ScanArray Express microarray scanner (Perkin Elmer) at 10-μm resolution and quantified using ScanArray Express software. The resulting data were normalized by total intensity, and median spot intensities were identified by using MIDAS (v. 2.22) software (71). The statistical analysis of microarray (SAM) algorithm (79) was conducted using the MeV program (v. 4.5.1) (71). Genes were considered to be significantly differentially regulated *in vivo* compared to *in vitro* if they were identified by SAM, had a median fold change value of at least 2-fold, and had a median spot intensity above background fluorescence. Genes that were differentially regulated over time were identified by using the Bayesian estimation of temporal regulation (BETR) algorithm (6) in MeV.

qRT-PCR. RNA was converted to cDNA by using the Superscript first-strand synthesis system (Invitrogen) according to the manufacturer's protocol. The resulting cDNA was confirmed to be free of chromosomal DNA contamination by PCR on samples with or without reverse transcriptase (RT) treatment. Samples were adjusted to a uniform concentration (4 or 6 ng/μl) by using a Nanodrop ND-1000 spectrophotometer. Each quantitative RT-PCR (qRT-PCR) was set up in duplicate and consisted of 30 ng cDNA template, 150 nM each primer, and 12.5 μl 2× SYBR green PCR master mix (Stratagene). Target genes were amplified with an Mx3000P thermal cycler (Stratagene). Melting curve analysis was used to confirm a lack of primer dimers, and no-template controls were used to ensure there was no genomic DNA contamination of reagents. Data were normalized to *rpoA* (RNA polymerase A) or *rpmC* (encodes 50S ribosomal protein L29) as specified and analyzed by the threshold cycle ($2^{-\Delta\Delta CT}$) method (43). Statistical analysis, including *t* tests and linear regression, was performed on $\log_2$-transformed data by using Prism software (GraphPad). Primer sequences will be provided upon request.

Mutant construction. An isogenic *gdhA* mutant was constructed by insertion of a kanamycin resistance cassette into the *gdhA* (PMI3008) coding sequence by the Targetron method (Sigma) as previously described (63). Basically, a group II intron was retargeted by PCR to specifically insert into *gdhA*. Intron insertion in *gdhA* was confirmed by PCR. The mutant was maintained on LB agar supplemented with kanamycin (25 μg/ml).

Preparation of crude protein extracts. *P. mirabilis* cells were grown in 1-liter flasks under the specified conditions for each experiment, harvested by centrifugation at 6,000 × *g* for 15 min, and resuspended in 5 ml buffer (for urease assays, 20 mM sodium phosphate buffer [pH 7.0], 1 mM EDTA, and 5 mM β-mercaptoethanol; for GDH and GS assays, 50 mM sodium phosphate buffer [pH 7.0]). Cells were disrupted by two 20,000-lb/in^2 passages through a French pressure cell press (American Instruments Company) and immediately placed on ice. The sample was cleared by centrifugation at 30,000 × *g* for 30 min at 4°C to remove insoluble material. The resulting cell extract was used as the enzyme source for activity measurements. Total protein concentration was determined using the bicinchoninic acid (BCA) assay (Thermo Scientific) according to the manufacturer's instructions, using bovine serum albumin as the standard.

Enzyme assays. Urease (EC 3.5.1.5) activity was determined by measuring released ammonia by the Berthelot reaction (24). Calibration curves used NH_4Cl as a standard. The reaction mixture contained 30 mM urea, 1 mM EDTA, 10 mM β-mercaptoethanol, and 20 mM sodium phosphate buffer (pH 7.5), in a total volume of 240 μl. The reaction was initiated by addition of 10-μl aliquots of various enzyme concentrations. After allowing the reaction to proceed for 5 to 10 min at room temperature, it was stopped by addition of 500 μl phenol-nitroprusside solution, 500 μl alkaline hypochlorite, and 2.5 ml of water, and color was allowed to develop for 5 min at room temperature. One unit of urease activity was defined as the amount of enzyme required to produce 1 μmol NH_3/min/ml. Jack bean urease (Sigma) was used as a positive control. Crude extracts of the *P. mirabilis* Δ*ureC* strain grown under the same conditions and similarly processed were used to measure background activity. Absorbance at 570 nm was measured with a BioSpec-1601 spectrophotometer (Shimadzu).

Glutamine synthetase (GS; EC 6.3.1.2) activity was assayed using the γ-glutamyltransferase assay as previously described (75). Activity was measured in imidazole buffer both in the presence of 0.4 mM Mn^{2+} at pH 7.38 (both adenylylated and unadenylylated enzymes are active under these conditions) and in the presence of 60 mM Mg^{2+} and 0.4 mM Mn^{2+} at pH 7.2 (only unadenylylated enzyme is active). The reaction buffer contained 0.15 mM glutamine, 4.1% neutral NH_2OH, 0.4 mM Na^+-ADP, and 2% $KAsO_4$ (pH 7.0) in 160 mM imidazole buffer (pH 7.4), and the divalent cation(s) in the concentrations specified above. The pH of the assay mix was adjusted according to the reaction. Briefly, 490-μl reactions were initiated by addition of 10-μl dilutions of crude *P. mirabilis* protein extract and allowed to proceed for 30 min at 37°C. The reaction was halted by addition of a stop mixture (3.3% $FeCl_3$, 2% trichloroacetic acid [TCA], 0.25 N HCl), and samples were briefly centrifuged at 4,000 × *g* to remove any precipitate. The production of γ-glutamylhydroxamate was determined at 540 nm in a Shimadzu BioSpec-1601 spectrophotometer. One unit of enzyme activity was defined as the amount of enzyme producing 1 μmol γ-glutamylhydroxamate/min/mg protein in the transfer reaction. Glutamine synthetase from *E. coli* (Sigma) was used as a positive control.

Glutamate dehydrogenase (EC 1.4.1.4) activity was measured in the forward (reductive amination activity) direction as described elsewhere (72). The reaction followed the oxidation of $NADPH_2$ spectrophotometrically at 340 nm and was monitored for 3 min at room temperature in a Genesys 10-S spectrophotometer (Thermo Scientific). The reaction mixture contained 100 mM Tris-HCl (pH 8.0), 100 mM NH_4Cl, 10 mM α-ketoglutarate, 0.1 mM $NADPH_2$, and appropriate dilutions of cell extracts in a total volume of 1 ml. Specific enzyme activity was calculated by using the $NADPH_2$ extinction coefficient of 6220 cm^{-1} M^{-1}. One unit of enzyme activity was defined as 1 μmol of coenzyme oxidized/min/ml. Crude extracts of the *P. mirabilis gdhA*Ω*kan* strain grown under the same conditions and similarly processed were used to measure background activity. Glutamate dehydrogenase from bovine liver (Sigma) was used as a positive control.

***In vivo* cochallenge.** Overnight cultures of wild-type *P. mirabilis* HI4320 and the isogenic *gdhA* mutant strain were individually adjusted to an estimated density of 2×10^8 CFU/ml (OD_{600} of 0.2). The *gdhA* mutant culture was mixed in a 1:1 ratio with the wild-type parent strain. Mice were transurethrally infected with a 50-μl suspension of the mixture (i.e., 1×10^7 CFU) as described above. At 7 days postinoculation, bladders, kidneys, and spleens were removed from euthanized mice, homogenized in 3 ml phosphate-buffered saline (PBS) using an OMNI mechanical homogenizer (OMNI International), and plated on LB medium or LB medium supplemented with kanamycin by using a spiral plater (Autoplate 4000; Spiral Biotech) to assess bacterial burden. Colony counts were enumerated using a Qcount (Spiral Biotech). Wild-type HI4320 infection was determined by subtracting the number of colonies on the kanamycin plate from the number of colonies on the plain LB plate. Statistical significance was assessed using the two-tailed Wilcoxon matched-pairs test. The competitive index (CI) was calculated by dividing the ratio of mutant to wild-type output CFU to the ratio of mutant to wild-type input CFU. CI values below 1 indicate outcompetition of the mutant by the wild-type parent.

Growth curves. Growth of bacterial strains was assessed with a Bioscreen C growth curve analyzer (Growth Curves, Ltd.). The optical density at 600 nm for triplicate cultures was measured at 15-min intervals. Cultures were maintained at 37°C with continuous shaking.

Microarray data accession number. Microarray data have been deposited in the Gene Expression Omnibus (GEO) database under series GSE25977.

RESULTS

Transcriptome of *Proteus mirabilis* in the murine urinary tract. Mice were transurethrally inoculated with *P. mirabilis*,

TABLE 1. The 50 genes most highly upregulated *in vivo* in this study

ORF[c]	Gene	Annotation	Rank[a]		Fold change[b]
			In vivo	*In vitro*	
PMI0263	*mrpA*	Major mannose-resistant/*Proteus*-like fimbrial protein	37	3,040	1,3806.33
PMI0264	*mrpB*	Fimbrial subunit	138	3,474	1,672.09
PMI0266	*mrpD*	Fimbrial chaperone protein	146	3,496	1,358.22
PMI0268	*mrpF*	Fimbrial subunit	218	2,905	1,227.47
PMI0271	*mrpJ*	Fimbrial operon regulator	191	2,688	904.14
PMI0269	*mrpG*	Fimbrial subunit	255	2,804	693.49
PMI0267	*mrpE*	Fimbrial subunit	272	3,018	616.84
PMI0265	*mrpC*	Fimbrial outer membrane usher protein	230	3,124	598.01
PMI0270	*mrpH*	Fimbrial adhesin	458	2,891	514.01
PMI3233		Putative membrane protein	350	2,194	344.22
PMI1706	*dmsB*	Anaerobic dimethyl sulfoxide reductase chain B	530	2,818	250.99
PMI0173		Hypothetical protein	547	2,892	232.47
PMI2673	*gntK*	Thermoresistant gluconokinase	537	3,125	220.23
PMI1205		Putative anaerobic dimethyl sulfoxide reductase chain B	533	2,487	210.95
PMI3234		Putative membrane protein	558	2,280	204.00
PMI1688		Putative di-/tripeptide transporter	546	2,490	183.19
PMI2969		Major facilitator superfamily transporter	503	2,286	167.77
PMI0730		Conserved hypothetical protein	514	1,973	161.35
PMI0249	*betU*	Putative secondary glycine betaine transporter	738	2,723	153.81
PMI0361		Putative phosphodiesterase	645	3,614	153.01
PMI2134	*agaA*	*N*-Acetylglucosamine-6-phosphate deacetylase	652	3,233	148.09
PMI1705	*dmsA*	Dimethyl sulfoxide reductase chain A	881	2,851	140.24
PMI0391		Putative sigma 54 modulation protein	493	2,108	131.78
PMI3232		Putative peptidase	403	1,924	122.47
PMI0973		Putative heat shock protein	930	2,728	122.19
PMI0706	*focA*	Probable formate transporter	568	1,898	122.12
PMI0187	*dsdA*	D-Serine dehydratase	909	1,990	121.54
PMI1568		Putative exported protease	620	2,266	119.64
PMI1406	*gadC*	Probable glutamate/γ-aminobutyrate antiporter	413	1,871	118.51
PMI2946		ABC transporter, permease protein	1,133	2,874	113.19
PMI3515		Phosphotransferase system IIBC component	1,003	3,455	108.08
PMI2672	*gntU*	Low-affinity gluconate transporter	797	2,149	102.07
PMI2948		Probable methyltransferase	661	2,215	100.26
PMI0287		Putative amidohydrolase/metallopeptidase	764	2,288	100.05
PMI2192		LuxR family transcriptional regulator	697	2,632	99.95
PMI0272		Probable transport protein	1,008	2,662	98.42
PMI3674		Probable aminohydrolase	813	2,423	97.48
PMI1601		Putative sodium:alanine symporter	664	2,278	96.94
PMI1725		Putative phage holin (lysis protein)	1,063	3,227	96.93
PMI3675		Putative C4-dicarboxylate transporter	931	2,866	92.96
PMI2292	*ptsG*	Phosphotransferase system, glucose-specific IIBC component	479	2,153	88.71
PMI2970		Putative membrane protein	854	2,925	88.61
PMI1707	*dmsC*	Anaerobic dimethyl sulfoxide reductase chain C	655	2,641	87.94
PMI2846	*dppB*	Dipeptide ABC transporter, permease protein	759	2,116	87.06
PMI2466		Putative plasmid-related protein	1,286	3,103	83.09
PMI0144		Putative ATP-binding protein	1,204	2,462	82.19
PMI2847	*dppA*	Dipeptide ABC transporter, substrate-binding protein	1,241	2,463	81.34
PMI1945	*ireA*	Putative TonB-dependent ferric siderophore receptor	722	2,667	78.99
PMI0434	*gltL*	Glutamate/aspartate ABC transporter, ATP-binding protein	1,048	2,580	74.90
PMI2529	*rpiB*	Putative ribose 5-phosphate isomerase	159	1,396	72.28

[a] Median expression rank across nine microarrays (including ribosomal genes): 1 is most highly expressed, and 3,719 is most weakly expressed.
[b] Median fold change *in vivo* compared to LB broth across nine microarrays.
[c] ORF, open reading frame.

and the infection was allowed to progress for 1 week. At 1, 3, and 7 days postinfection, transcription of bacteria in pooled voided mouse urine was measured by microarray and compared to transcription by *P. mirabilis* cultured to the logarithmic phase in LB broth. LB broth was selected for the *in vitro* condition, despite its complexity, for three reasons. LB broth represents a common laboratory medium for culture of enteric bacteria, the use of this medium allowed comparison to the only other *in vivo* transcriptome of a uropathogen, *E. coli* (74), and culture of *P. mirabilis* in urine *ex vivo* is cidal for the urease-producing bacterium.

At 7 days postinfection, there is a typical median of 1×10^6 to 1×10^7 CFU/ml in urine. Three independent microarrays were analyzed for each time point. To understand the overall pattern of gene expression *in vivo*, all nine microarrays were analyzed together. There were 471 genes significantly upregulated *in vivo* compared to *in vitro*, and there were 82 genes significantly downregulated *in vivo*. Table 1 lists the

TABLE 2. The 50 nonribosomal genes most highly expressed *in vivo* in this study

ORF[c]	Gene	Annotation	Rank[a]		Fold change[b]
			In vivo	*In vitro*	
PMI1035		Translation initiation factor IF-3	9	3	−1.33
PMI0765	*ompF*	Outer membrane porin	13	3	−1.25
PMI3251	*tufB*	Elongation factor Tu	13	6	−1.23
PMI3275	*secY*	Preprotein translocase SecY subunit	23	20	1.03
PMI3280	*rpoA*	DNA-directed RNA polymerase alpha chain	26	19	−1.32
PMI2792	*tufB*	Elongation factor Tu	28	29	−1.16
PMI0856		Conserved hypothetical protein	29	36	−1.85
PMI0862	*acpP*	Acyl carrier protein	33	16	−1.66
PMI0263	*mrpA*	Major mannose-resistant/*Proteus*-like fimbria	37	3,040	13,806.33
PMI0785	*ompA*	Outer membrane protein A	37	50	1.21
PMI1676	*cspC*	Cold shock-like protein	39	9	−2.09
PMI2771	*hupA*	DNA-binding protein HU-alpha (HU-2)	52	60	−1.39
PMI3375	*priB*	Primosomal replication protein N	52	34	−1.61
PMI2793	*fusA*	Elongation factor G (EF-G)	52	80	1.17
PMI0716	*ihfB*	Integration host factor beta-subunit	57	53	−1.25
PMI0384	*rimM*	16S rRNA processing protein	59	59	−1.28
PMI2284	*tsf*	Elongation factor Ts	59	75	−1.00
PMI3059	*atpE*	ATP synthase C chain	59	57	−1.47
PMI1213	*ahpC*	Alkyl hydroperoxide reductase subunit C	62	165	6.14
PMI3062	*atpA*	ATP synthase alpha chain	62	68	−1.07
PMI3415	*secG*	Protein export membrane protein	66	71	−1.05
PMI0073	*ahpC*	Putative alkyl hydroperoxide reductase	67	104	1.83
PMI3063	*atpG*	ATP synthase gamma chain	68	70	−1.14
PMI0385	*trmD*	tRNA (guanine-N1)-methyltransferase	69	65	−1.69
PMI0585	*pal*	Peptidoglycan-associated lipoprotein	71	46	−2.60
PMI3060	*atpF*	ATP synthase B chain	71	60	−1.39
PMI1504	*gapA*	Glyceraldehyde 3-phosphate dehydrogenase A	72	81	1.33
PMI0118	*hupB*	DNA-binding protein HU-beta	75	76	−1.70
PMI3064	*atpD*	ATP synthase beta chain	75	69	−1.18
PMI3065	*atpC*	ATP synthase epsilon chain	78	84	−1.22
PMI3061	*atpH*	ATP synthase delta chain	81	83	−1.15
PMI2544	*groS*	10-kDa chaperonin	82	66	−1.26
PMI3057	*atpI*	ATP synthase protein I	82	85	−1.35
PMI3296		Conserved hypothetical protein	83	96	−1.11
PMI0418	*cspE*	Putative cold shock protein	84	69	−2.52
PMI0861	*fabG*	3-Oxoacyl-[acyl-carrier protein] reductase	85	79	−1.67
PMI1039	*pheT*	Phenylalanyl-tRNA synthetase beta chain	93	103	1.06
PMI2784	*rpoC*	DNA-directed RNA polymerase beta′ subunit	93	95	−1.15
PMI1898	*grcA*	Autonomous glycyl radical cofactor	95	788	19.18
PMI3622	*fis*	DNA-binding protein Fis	96	90	−1.37
PMI1034	*thrS*	Threonyl-tRNA synthetase	96	90	−1.27
PMI0114	*tig*	Trigger factor	98	98	−1.15
PMI1828	*ptsH*	Phosphotransferase system phosphocarrier protein	100	683	16.77
PMI1488	*hns*	DNA-binding protein (histone-like structuring protein)	100	93	−1.41
PMI3364	*miaA*	tRNA delta(2)-isopentenylpyrophosphate transferase	102	137	−1.11
PMI2833		Putative endoribonuclease	103	124	−1.02
PMI0842		TonB-dependent receptor	104	913	17.18
PMI3058	*atpB*	ATP synthase A chain	106	77	−1.66
PMI0243	*fbaA*	Fructose-bisphosphate aldolase class II	110	144	1.61
PMI0691	*infA*	Translation initiation factor IF-1	111	101	−1.60

[a] Median expression rank across nine microarrays (including ribosomal genes): 1 is most highly expressed, and 3,719 is most weakly expressed.
[b] Median fold change *in vivo* compared to LB broth across nine microarrays.
[c] ORF, open reading frame.

top 50 genes upregulated *in vivo*, Table 2 lists the 50 nonribosomal genes most highly expressed *in vivo*, and Table 3 lists the 50 genes most downregulated *in vivo*. The complete lists of differentially regulated genes are found in Tables S1 and S2 in the supplemental material. The genes encoding mannose-resistant *Proteus*-like (MR/P) fimbriae were very highly expressed *in vivo*; the nine genes comprising the *mrp* operon (40) were the nine most upregulated genes *in vivo* (Table 1). Indeed, *mrpA*, the gene encoding the major structural subunit of MR/P fimbriae, was the ninth most highly expressed nonribosomal gene *in vivo* (Table 2). Major classes of genes upregulated *in vivo* encode amino acid and carbohydrate transporters, energy production and conversion proteins, and ion transport (predominantly iron) proteins (Table 4). Genes encoding cell motility proteins were the most highly downregulated genes *in vivo*; 19 of the 50 most downregulated genes encoded flagellar components and chemotaxis proteins (Table 3). Major classes of genes downregulated *in vivo*, of which cell motility genes are the largest defined category, are depicted in Table 4.

Virulence gene expression. Regulation of genes previously identified in *P. mirabilis* virulence was specifically examined (Fig. 1). As mentioned, the *mrp* operon is both highly upregu-

TABLE 3. The 50 genes most highly downregulated *in vivo* in this study

ORF[c]	Gene	Annotation	Rank[a]		Fold change[b]
			In vivo	*In vitro*	
PMI1629	*fliE*	Flagellar hook-basal body complex protein	2,748	492	−88.25
PMI0994		Putative lipoprotein	2,785	506	−70.63
PMI1654	*flgB*	Flagellar basal-body rod protein	2,254	465	−47.91
PMI1618	*fliA*	RNA polymerase sigma factor for flagellar operon	1,448	136	−39.10
PMI1651	*flgE*	Flagellar hook protein	2,232	439	−35.30
PMI1877	*pmfA*	Major fimbrial subunit	671	66	−29.64
PMI1650	*flgF*	Flagellar basal-body rod protein	1,943	435	−23.85
PMI1096		2-Oxoglutarate and Fe(II)-dependent oxygenase superfamily protein	1,794	243	−21.27
PMI1636	*fliL*	Flagellar protein FliL	2,049	503	−20.33
PMI1649	*flgG*	Flagellar basal-body rod protein (distal rod protein)	1,716	502	−20.03
PMI0993		Putative lipoprotein	2,330	540	−19.98
PMI1653	*flgC*	Flagellar basal-body rod protein	2,525	703	−19.72
PMI1644	*flgL*	Flagellar hook-associated protein 3 (hook-filament junction protein)	2,323	674	−19.41
PMI0488		Putative phage membrane protein	1,245	394	−19.10
PMI1941		Conserved hypothetical protein	2,460	1,084	−18.60
PMI2109	*mgtE*	Magnesium transporter	1,769	412	−15.85
PMI1638	*fliN*	Flagellar motor switch protein	2,409	710	−15.41
PMI1637	*fliM*	Flagellar motor switch protein	2,410	679	−15.38
PMI2814		RpiR-family transcriptional regulator	2,364	873	−15.02
PMI3177	*kbl*	2-Amino-3-ketobutyrate coenzyme A ligase	1,871	471	−12.99
PMI1631	*fliG*	Flagellar motor switch protein	2,449	704	−12.48
PMI1469	*fim8A*	Fimbrial subunit	1,787	593	−11.97
PMI0022		Putative cell killing protein	1,859	441	−11.88
PMI1595	*pagP*	Putative antimicrobial peptide resistance and lipid A acylation protein	1,662	550	−10.92
PMI1622	*fliS*	Flagellar protein FliS	1,825	905	−10.83
PMI0291	*treB*	Phosphotransferase system, trehalose-specific IIBC component	2,792	941	−10.65
PMI0596		Putative membrane protein	1,338	174	−10.58
PMI1656	*flgM*	Negative regulator of flagellin synthesis	1,614	718	−10.24
PMI3178	*tdh*	L-Threonine 3-dehydrogenase	1,464	482	−10.21
PMI1943		Major facilitator superfamily transporter	1,415	207	−10.15
PMI1620	*flaA*/*fliC1*	Flagellin 1	750	108	−9.59
PMI1666	*cheD*	Methyl-accepting chemotaxis protein	2,481	936	−9.53
PMI1645	*flgK*	Flagellar hook-associated protein 1	2,057	807	−9.29
PMI0044		Putative outer membrane protein	1,442	363	−8.33
PMI1621	*flaD*/*fliD*	Flagellar hook-associated protein 2	2,306	1,261	−8.29
PMI3211	*glpF*	Glycerol uptake facilitator protein	1,171	217	−7.52
PMI1506	*mipA*	MltA-interacting protein precursor	566	107	−7.37
PMI1879	*pmfD*	Fimbrial chaperone protein	1,504	659	−6.98
PMI1489	*wbnF*	Probable nucleotide sugar epimerase	1,730	387	−6.98
PMI1617	*fliZ*	FliZ protein	979	240	−5.85
PMI1061	*fim5A*	Fimbrial protein	1,945	752	−5.51
PMI2203		Putative isochorismatase	1,828	799	−5.42
PMI0580		Putative thioesterase	1,432	550	−4.99
PMI2093	*speB*	Agmatinase	853	172	−4.98
PMI2094	*speA*	Biosynthetic arginine decarboxylase	898	285	−4.93
PMI0582	*tolR*	Biopolymer transport protein	1,280	379	−4.77
PMI1958		Putative DNA-damage-inducible protein	1,436	658	−4.31
PMI2930	*glpD*/*glyD*	Aerobic glycerol-3-phosphate dehydrogenase	458	97	−3.96
PMI0682	*artP*	Arginine ABC transporter, ATP-binding protein	470	187	−3.74
PMI1286	*osmB*	Osmotically inducible lipoprotein	1,692	925	−3.68

[a] Median expression rank across nine microarrays (including ribosomal genes): 1 is most highly expressed, and 3,719 is most weakly expressed.
[b] Median fold change *in vivo* compared to LB broth across nine microarrays.
[c] ORF, open reading frame.

lated (Fig. 1) and highly expressed *in vivo*. However, *pmfA*, which encodes the major structural subunit of *Proteus mirabilis* fimbriae (PMF), was downregulated *in vivo* despite having a role in bladder (49, 86) and kidney (86) colonization in mice. Genes coding for two other fimbriae, previously identified as virulence factors by signature-tagged mutagenesis (12, 26), were either downregulated (*fim8A*) or upregulated (*fim14A*), although neither was highly expressed *in vivo*. Genes encoding three *P. mirabilis* toxins, *zapA* (44, 83), hemolysin *hpmA* (77), and *pta* (*Proteus* toxic agglutinin) (2), were expressed at approximately background levels *in vivo* and were inconsistently upregulated. The entire urease operon, which is induced in the presence of urea, was both highly expressed and highly upregulated *in vivo*. Peptide transporter genes *dppA* and *oppA*, which have been implicated in virulence for both *P. mirabilis* (64) and UPEC (4), were upregulated *in vivo*; iron uptake genes (*exbBD*, *sitABC*, *hmuST*, *ireA*, *nrpY*, *feoAB*, PMI0331, PMI0363, PMI0842, PMI1424, PMI1437, and PMI2957 to PMI2960) were similarly upregulated.

Other genes of interest that were upregulated *in vivo* in-

TABLE 4. Categories of genes differentially regulated *in vivo*

Category	No. of genes:	
	Upregulated *in vivo*	Downregulated *in vivo*
Amino acid transport and metabolism	58	7
Carbohydrate transport and metabolism	37	4
Cell cycle control, cell division, and chromosome partitioning	6	0
Cell motility	0	19
Cell wall/membrane/envelope biogenesis	19	9
Coenzyme transport and metabolism	17	3
Defense mechanisms	1	0
Energy production and conversion	50	4
Fimbriae	10	4
Function unknown	57	12
General function prediction only	42	4
Inorganic ion transport and metabolism	41	2
Intracellular trafficking, secretion, and vesicular transport	2	1
Lipid transport and metabolism	6	0
Nucleotide transport and metabolism	17	0
Phage and mobile element	20	1
Posttranslational modification, protein turnover, and chaperones	24	2
Replication, recombination, and repair	19	1
Secondary metabolite biosynthesis, transport, and catabolism	4	1
Signal transduction mechanisms	5	0
Transcription	25	3
Translation, ribosomal structure, and biogenesis	12	5

cluded pyruvate metabolism genes (*aceEF*, *pta*, *ackA*, *poxB*, *pflB*, and *dsdA*), genes likely involved in osmoprotection (*betU*, *putP*, *gltS*, *gltL*, and *gadC*), and eight genes within the previously identified mobile integrated and conjugative element ICE*Pm1* (PMI2568, PMI2573, PMI2595, PMI2598, PMI2608, PMI2627, PMI2628, and PMI2629) (18).

Temporal gene regulation. Microarrays were also analyzed separately at each time point (1, 3, and 7 days postinfection), and some temporal regulation was noted. At 1 day postinfection, 93 genes were significantly upregulated *in vivo*; 5 genes were downregulated. At 3 days postinfection, 294 genes were upregulated and 6 were downregulated. At 7 days postinfection, 204 genes were upregulated and 1 gene was downregulated (data not shown). The BETR algorithm identified three groups of genes that were differentially regulated over time (Fig. 2). The first group consists of genes that were highly induced *in vivo* at day 1 but by day 7 were less upregulated (Fig. 2A). This group of seven genes included three genes from the *mrp* operon (*mrpA*, *mrpE*, and *mrpH*). Three other genes in this group are predicted to encode transporters (PMI0272 and PMI2947), including a putative di-/tripeptide transporter (PMI1688). The second group of genes was repressed at day 1 but by day 7 had similar expression compared to genes from cells cultured in LB broth (Fig. 2B). Of the 10 genes in group 2, 5 encode flagellar components (*fliN*, *flgD*, *fliH*, *flhD*, and *flgL*). Three genes in this group encode putative lipoproteins (PMI0977, PMI0994, and PMI1840). The third group consisted of genes that were either slightly repressed or not differentially regulated at day 1 but were induced at day 7 (Fig. 2C). There were eight genes in this group, including the transcriptional regulator *hexA*.

Validation of the microarrays by qRT-PCR. Expression of 15 genes that were found to be differentially regulated by microarray *in vivo* compared to LB was also measured by qRT-PCR (Fig. 3A). Urine collected from mice 3 days postinfection was used as the *in vivo* source of RNA. Microarray and qRT-PCR data were in agreement for 13 of the 15 genes, including the very strong *in vivo* upregulation of *mrpA*. Two genes predicted to be upregulated *in vivo* by microarray, *ipaD* and PMI2192, were either downregulated (*ipaD*) or not differentially regulated (PMI2192) by qRT-PCR. To test the concordance of microarray and qRT-PCR data, the $\log_2$-transformed fold changes were plotted against one another (Fig. 3B). Linear regression calculations confirmed the significant agreement between microarray and qRT-PCR data (r^2 = 0.5186, P = 0.0025).

Glutamate dehydrogenase is upregulated during urinary tract infection. Ammonia is the preferred nitrogen source for enteric bacteria. The two primary ammonia incorporation sys-

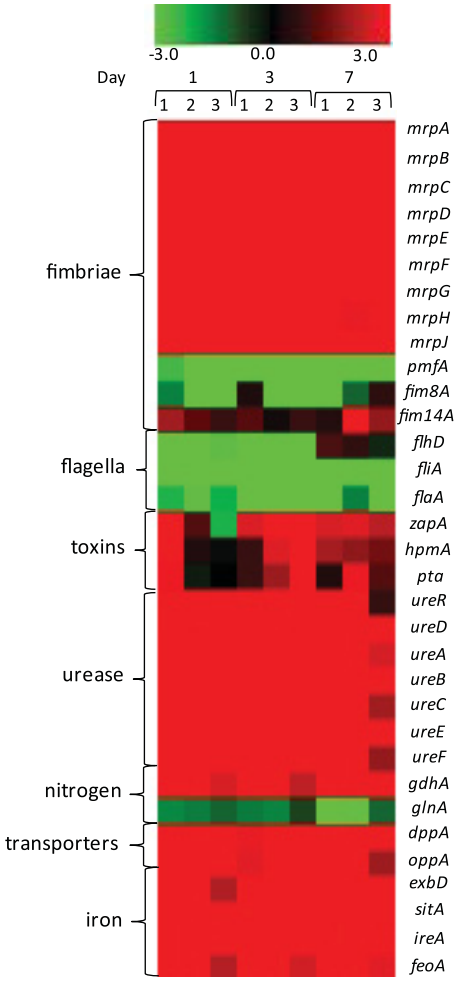

FIG. 1. Heat map of expression data for specific virulence-associated genes, depicting the ratio of expression in LB broth versus *in vivo*. The legend at the top indicates the color associated with $\log_2$ fold change: red, upregulated *in vivo*; green, downregulated *in vivo*; black, not differentially regulated.

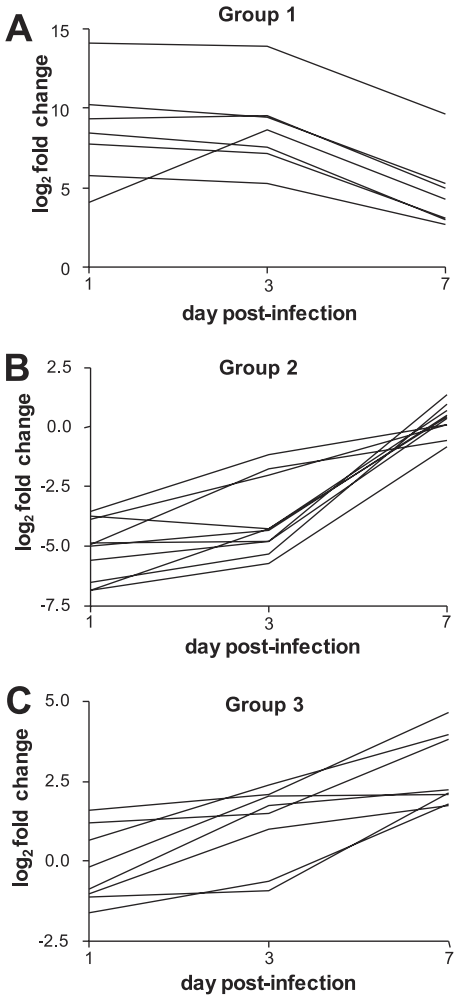

FIG. 2. *P. mirabilis* genes are temporally regulated *in vivo*. Nine microarrays were analyzed for differential regulation of genes over time using the BETR algorithm. (A) Group 1 genes were highly induced *in vivo* at day 1 but less highly expressed by day 7. (B) Group 2 genes were repressed *in vivo* at day 1 but were not differentially expressed compared to *in vitro* at day 7. (C) Group 3 genes were either slightly repressed or not differentially regulated at day 1, but were induced at day 7.

tems, *gdhA* (PMI3008; glutamate dehydrogenase [GDH]) and *glnA* (PMI2882; glutamine synthetase [GS]), were inversely regulated *in vivo*, with *gdhA* upregulated 10.75-fold and *glnA* downregulated 2.78-fold (Fig. 1). The opposite result was observed for UPEC *in vivo*, in which *gdhA* was slightly downregulated (1.75-fold) and *glnA* was upregulated 12-fold (74). Glutamine synthetase is the primary ammonia uptake system when nitrogen levels are limited, while glutamate dehydrogenase confers ammonia uptake when ammonia levels are high or, correspondingly, when energy is limited (25).

Nitrogen assimilation appears to be handled differently by *P. mirabilis* than UPEC during UTI based on microarray and qPCR data assessing transcription. However, because nitrogen assimilation can be regulated posttranslationally as well as transcriptionally, we attempted to correlate the transcript levels of urease, GDH, and GS with the enzyme activities of these gene products (see below).

GDH is not upregulated in excess ammonia alone. To define *in vitro* culture conditions that yielded *in vivo* gene expression patterns, we conducted a series of experiments. Upregulation of *gdhA* and repression of *glnA in vivo* by *P. mirabilis* suggested that ammonia incorporation drives the expression of these genes in *P. mirabilis.* To test the effect of nitrogen availability on *gdhA* and *glnA* gene expression, *P. mirabilis* HI4320 was cultured in LB broth with or without 500 mM NH_4Cl. As assessed by qRT-PCR (Fig. 4A), *gdhA* was not upregulated; however, as expected, *glnA* was downregulated. Similar results were obtained by using NH_4Cl concentrations ranging from 100 mM to 1 M (data not shown). As assessed by enzyme activity (Fig. 4B), GDH was also not significantly upregulated when *P. mirabilis* was cultured in 500 mM NH_4Cl. GS enzyme activity was downregulated under this condition. Therefore, in this experiment, transcription, as assessed by microarray and qRT-PCR, serves as a proxy for enzyme activity. NH_4Cl, however, in this experiment was supplied exogenously, while *in vivo*, urea in urine is hydrolyzed to ammonia by intracellular urease. Therefore, *P. mirabilis* was also cultured in LB broth supplemented with 400 mM urea (within the normal human physiological concentration range for urine). Again, *gdhA* (Fig.

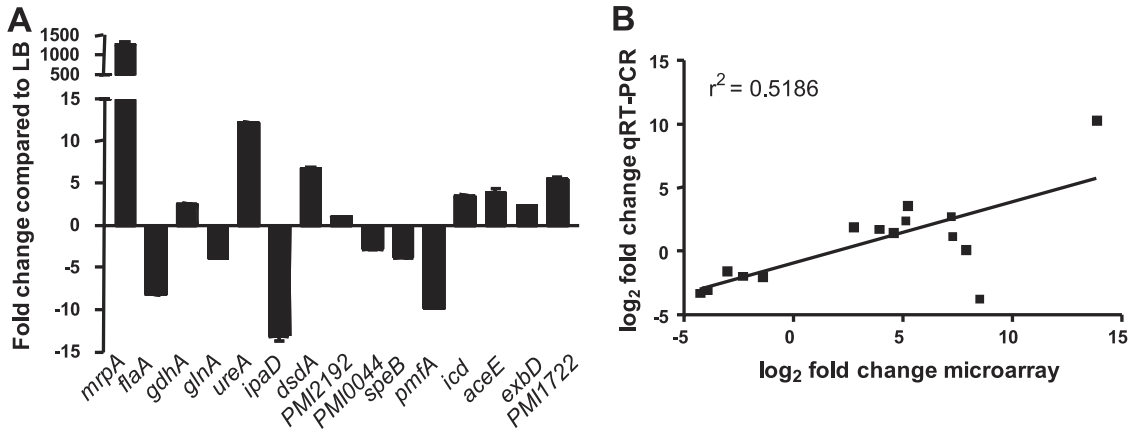

FIG. 3. qRT-PCR validation of *in vivo* microarrays. (A) Expression of 15 genes *in vivo* compared to during logarithmic-phase growth in LB culture as measured by qRT-PCR. (B) Concordance of microarray and qRT-PCR data for the 15 genes depicted in panel A. The $\log_2$-transformed fold change values are plotted, with linear regression shown. Median fold change at 3 days was used for the microarray data points. The r^2 value is 0.5186, and the slope has a significant deviation from zero ($P = 0.0025$).

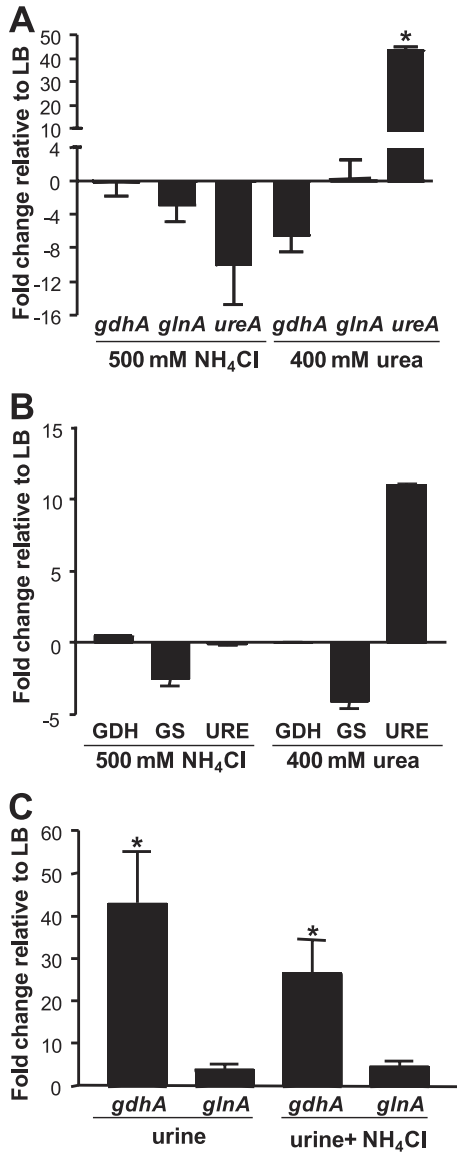

FIG. 4. Exogenous nitrogen is not the driving force behind *in vivo* *gdhA* and *glnA* expression. (A) RNA was isolated from *P. mirabilis* HI4320 cultured in LB supplemented with either 500 mM NH_4Cl or 400 mM urea. No significant changes in *gdhA* or *glnA* were found by qRT-PCR in comparison to unsupplemented LB. However, addition of urea significantly upregulated expression of *ureA*. (B) Enzyme activities were determined for whole-cell lysates of *P. mirabilis* HI4320 cultured under identical conditions to those described for panel A. Glutamate dehydrogenase (GDH), total glutamine synthetase (GS), and urease (URE) enzyme activities (average of five technical replicates) were measured and expressed as fold change relative to preparations from *P. mirabilis* cultured in LB broth. (C) A *ureC* mutant was cultured in LB broth or pooled human urine with or without 100 mM NH_4Cl, and expression of *gdhA* and *glnA* was measured by qRT-PCR. (A and C) Expression was normalized to *rpoA*. At least three independent experiments were conducted for each condition tested. Error bars represent standard errors of the mean. *, $P < 0.05$.

4A) and GDH enzyme activity (Fig. 4B) were not upregulated compared to those in the cells cultured in LB broth, although urease gene *ureA* expression (mean of 43.5-fold) and urease enzyme activity were highly upregulated during culture in urea (Fig. 4A and B). The pH of the urea culture was approximately 8.5 at the time bacteria were harvested, as a consequence of urease activity.

To assess whether a component in urine might contribute to the differential expression of *gdhA* and *glnA*, we used a *ureC* mutant that is unable to make functional urease (33) and therefore does not increase the pH of urea-containing cultures. This mutant was cultured to the logarithmic phase in pooled human urine with or without 100 mM NH_4Cl supplementation. Compared to *ureC* cells cultured in LB, *gdhA* was significantly upregulated in urine with or without NH_4Cl (38.6-fold and 24.5-fold, respectively) (Fig. 4C). However, *glnA* was not differentially regulated. These data suggest that upregulation of *gdhA* *in vivo* was not due to ammonia excess *per se* and that some other undefined factor was regulating *gdhA* and *glnA*.

High osmolarity alone does not induce GDH. Because *gdhA* and *glnA* were expressed differentially between *P. mirabilis* and UPEC *in vivo*, we sought to determine additional differences in the physiology of these species that might provide clues regarding this pattern of gene expression. Urine is generally hyperosmotic, averaging 500 to 800 mosmol/kg in humans and 1,040 mosmol/kg in female CBA mice (21), which can interfere with bacterial growth (7). In addition, glutamate, a product of *gdhA* upregulation, may be used to buffer against osmotic stress (reviewed in reference 45). Thus, *P. mirabilis* HI4320 and *E. coli* CFT073 were each cultured in LB supplemented with NH_4Cl over a range of 0 to 1 M. While growth was similar for *P. mirabilis* and *E. coli* at lower salt concentrations, *E. coli* was unable to grow at 1 M NH_4Cl (Fig. 5A). In contrast, *P. mirabilis* growth in 1 M NH_4Cl was only slightly retarded compared to that at lower salt concentrations (Fig. 5A). However, because *gdhA* is not upregulated in 500 mM NH_4Cl (Fig. 4A) or 1 M NH_4Cl (data not shown), osmotic buffering was ruled out as the sole cause for differential gene expression in *P. mirabilis* and *E. coli*.

***P. mirabilis* uses citrate as a carbon source, while UPEC does not.** Citrate, secreted in human urine at a rate of 3 to 20 mg/kg/day (5), is also a key intermediate of the TCA cycle and was a candidate carbon source that upregulates *gdhA*. Most *P. mirabilis* strains can use citrate as the sole carbon source (29), while most *E. coli* strains cannot. To test whether *P. mirabilis* HI4320 and *E. coli* CFT073 differ in their ability to use specific carbon sources, both strains were cultured in minimal medium supplemented with 1% glycerol, citrate, or acetate. *P. mirabilis* HI4320 was able to use all three carbon sources, while UPEC strain CFT073 was unable to utilize citrate (Fig. 5B).

A *gdhA* mutant has a growth defect in minimal medium containing citrate as the sole carbon source. Opposing regulation of *gdhA* in *P. mirabilis* and *E. coli*, coupled with differing abilities to utilize citrate, led us to hypothesize that GDH might play a unique role in central metabolism for *P. mirabilis.* Therefore, *gdhA* was inactivated by insertion of a targeted transposon, and the ability of the mutant to grow in rich and minimal media was compared to that of the wild-type isogenic parent strain (Fig. 5C). The *gdhA* mutant displayed a slight growth defect in minimal medium with glycerol as a carbon source but a more pronounced defect when citrate was the sole carbon source (Fig. 5C). As with *E. coli* (68), there was no difference in growth rates of wild-type *P. mirabilis* and the *gdhA* mutant in LB broth.

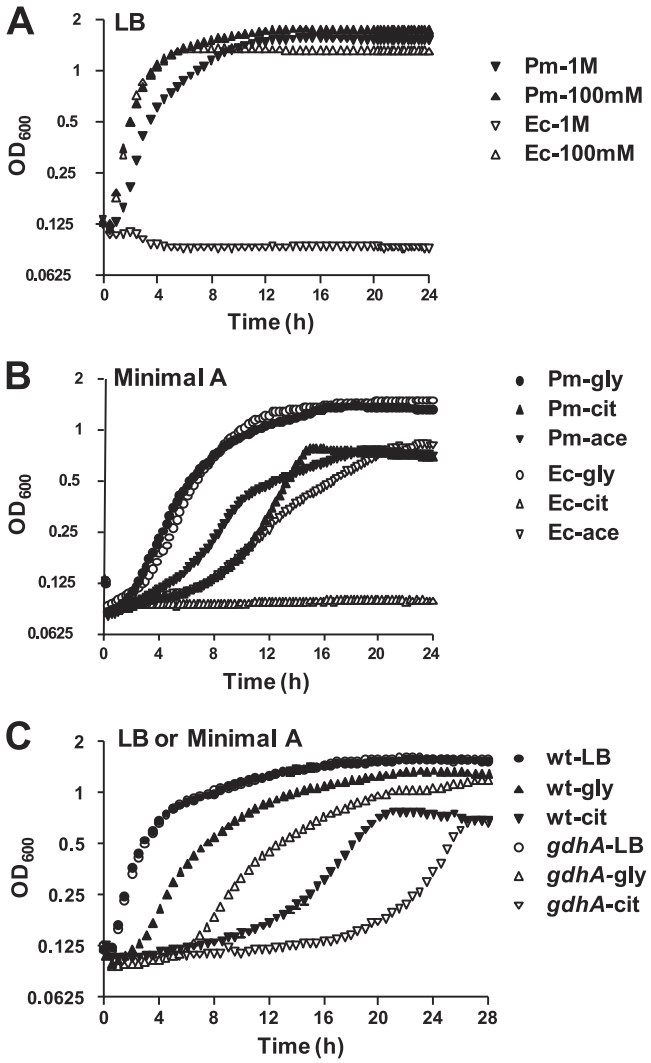

FIG. 5. Comparison of growth of *P. mirabilis* HI4320 (Pm) and *E. coli* CFT073 (Ec) under high-osmolarity conditions or with specific carbon sources. (A) LB broth supplemented with either 100 mM or 1 M NH_4Cl; (B) minimal A medium with 1% glycerol, citrate, or acetate as the carbon source; (C) *P. mirabilis* HI4320 and HI4320 *gdhA*Ω*kan* cultured in LB broth or minimal A medium with glycerol or citrate as the carbon source. At least three independent experiments were conducted for each condition tested; one representative experiment with three technical replicates is shown.

Culture in citrate recapitulates *in vivo* nitrogen gene expression patterns. Since *P. mirabilis gdhA* expression is increased *in vivo*, and a *gdhA* mutant has a growth defect when cultured in minimal medium with citrate as a carbon source, we postulated that citrate could be directly affecting expression of ammonia incorporation genes *gdhA* and *glnA*. Therefore, wild-type *P. mirabilis* was cultured to the mid-logarithmic phase in LB or minimal medium, and gene expression of *gdhA* and *glnA* was measured by qRT-PCR. Expression of *gdhA* (Fig. 6A) and GDH enzyme activity (Fig. 6B) were significantly increased in all three carbon sources tested (glucose, glycerol, and citrate) compared to the levels in LB broth, but *glnA* expression was significantly decreased only when citrate was used as the carbon source (Fig. 6A). GS enzyme activity was also lower in citrate than in glucose or glycerol (Fig. 6B). Thus, culture in citrate mimics *in vivo* conditions with respect to the expression pattern of *gdhA* and *glnA*.

***gdhA* contributes to *in vivo* fitness of *P. mirabilis*.** Based on the experiments described above, we hypothesized that GDH plays a central metabolic role during infection of the urinary tract. To test this, the *gdhA* mutant was mixed 1:1 with the isogenic parent strain and transurethrally inoculated into the bladders of 10 mice. After 7 days, the bacterial burdens of the *gdhA* mutant and wild type were enumerated in the bladders, kidneys, and spleens of these mice. As assessed by the competitive indices, the *gdhA* mutant was defective in colonization of all three sites tested ($P < 0.05$) (Fig. 7), suggesting that GDH is necessary for *P. mirabilis* fitness in the urinary tract, perhaps serving as a checkpoint for intracellular carbon and nitrogen levels.

DISCUSSION

This is the first microarray analysis of transcription by an agent of complicated UTI during an infection, as well as the first study examining global temporal control of bacterial gene expression during UTI. Previous studies have examined gene expression by *E. coli* during UTI in mice (74), in humans with asymptomatic bacteriuria (70), and in patients with UTI (22). There are several similarities in gene expression by *P. mirabilis* and *E. coli* during UTI. Both *P. mirabilis* and *E. coli* activate systems involved in iron uptake, pyruvate catabolism, peptide uptake, and osmoprotection. Both species have robust metabolism *in vivo*, as indicated by high expression of ribosomal genes. *P. mirabilis* and UPEC each upregulate a specific fimbrial operon *in vivo* (*mrp* and *fim*, respectively), although the upregulation of *mrp* is much stronger than that of *fim* (13,806-fold versus 7.82-fold for *mrpA* and *fimA*, respectively). Likewise, both pathogens downregulate flagellar and chemotaxis genes *in vivo*.

P. mirabilis in vivo global gene expression not only was verified by qRT-PCR but also agrees with previous reports on *P. mirabilis* virulence. Genes encoding MR/P fimbriae were the most highly upregulated genes *in vivo*, with the major structural gene *mrpA* upregulated 13,800-fold (median). Previous studies have shown that increased expression of MR/P fimbriae correlates with higher levels of colonization in the mouse bladder (36), the majority of bacteria in the bladder and ureters express MR/P fimbriae (31), and an *mrp* mutant is attenuated in the mouse model of ascending UTI (8). Furthermore, vaccine trials in mice using intact MR/P fimbriae (39) or recombinant components of MR/P fimbriae (38, 39, 73) reduce bacterial burden after challenge. Expression of MR/P fimbriae has not been tested during human infection; this experiment will be critical to future vaccine efforts since UPEC highly expresses type I fimbriae in mice (56, 74), and these fimbriae are required for virulence in mice (14, 46), but type I fimbriae are not well expressed or possibly transiently expressed during human UTI (22). The last gene of the *mrp* operon, *mrpJ*, encodes a transcriptional repressor of flagella (40). The high expression of this gene *in vivo* is consistent with reduced expression of flagella during murine UTI. Interestingly, the *mrp* operon upregulation is highest at days 1 and 3 postinfection (*mrpJ* median of 1,189-fold upregulated), and less at day 7 (*mrpJ* median

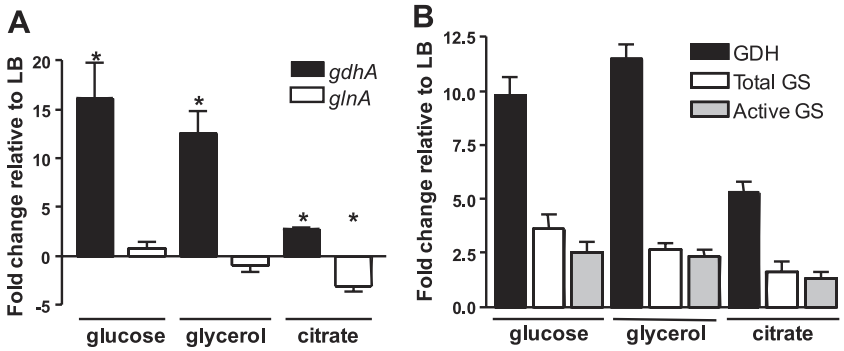

FIG. 6. Citrate as the sole carbon source drives *in vivo* expression patterns of *gdhA* and *glnA*. (A) *P. mirabilis* HI4320 was cultured in LB or minimal A medium with glucose, glycerol, or citrate as the carbon source. qRT-PCR analysis of RNA revealed upregulation of *gdhA* in minimal A medium with all three carbon sources, but *gdhA* was only downregulated when citrate was used as the carbon source. At least three independent experiments were conducted for each condition tested. Expression of *rpoA*, routinely used for normalization of gene expression by *P. mirabilis*, was decreased in minimal medium relative to LB; therefore, *rpmC* was used to normalize expression in these experiments. *, $P < 0.05$. (B) Enzyme activities were determined for whole-cell lysates of *P. mirabilis* HI4320 cultured under identical conditions to those described for panel A. Glutamate dehydrogenase (GDH), total glutamine synthetase (GS), and unadenylylated (active) GS enzyme activities (average of five technical replicates from each of two independent preparations) were measured and expressed as fold change relative to preparations from *P. mirabilis* cultured in LB.

of 126-fold upregulated); at the same time, the repression of flagellar genes may be easing by day 7. (The flagellar master regulator *flhD* is downregulated a median of 12.5-fold at days 1 and 3 and upregulated a median of 1.59-fold at day 7.) Additionally, another regulator of flagellum-mediated motility, *hexA* (64), was upregulated at day 7. These data suggest a potential increased role for flagella and corresponding lesser role for MR/P fimbriae at this later stage in the disease process. During experimental UPEC UTI, flagellar genes are transiently upregulated 4 h postinfection, when the bacteria are ascending the ureters from the bladder to the kidneys (35). It will be useful to examine *P. mirabilis* fimbrial and flagellar gene expression at early time points (less than 24 h), as well as to study global temporal gene transcription during UPEC UTI.

Other genes found to be upregulated *in vivo* also agree with single-gene-knockout virulence studies. Iron uptake systems upregulated *in vivo* are required for colonization (*hmuR2*) (42) and virulence (*pbtA*) (27) in mice, and many are immunogenic (PMI0409, PMI0842, *hmuR2*, *ireA*, and PMI2596) (58). Zinc uptake systems are also required for virulence (59), are immunogenic in mice (58), and were upregulated *in vivo*. Likewise, urease, a well-documented virulence factor for *P. mirabilis* (12, 20, 32, 33, 54), was upregulated. Toxin genes (*hpmA*, *zapA*, and *pta*) were a notable exception; these genes were expressed at or below background levels both *in vitro* and *in vivo*. It is possible that expression of these genes is more localized to specific sites in the urinary tract or that subtle changes in transcript level lead to much larger changes in protein activity. Two classes of genes which are involved with virulence were downregulated *in vivo*: flagella and PMF fimbriae. Flagella are energetically expensive to construct and maintain; they also activate innate immune response via Toll-like receptor 5 (17). Thus, flagellar regulation is likely tightly controlled *in vivo*, much as it is temporally controlled during experimental UPEC UTI (35). The role of PMF fimbriae is unknown at this time, although knockout studies have shown these fimbriae are required for full virulence (49, 86, 87), and components of PMF fimbriae have been successfully used in experimental vaccines (73). It is possible these fimbriae are required for adherence to specific tissues, which prevents PMF-expressing bacteria from being shed into the urine. Alternatively, like flagella, PMF fimbriae are only required during a limited time during UTI progression and may be tightly regulated *in vivo*.

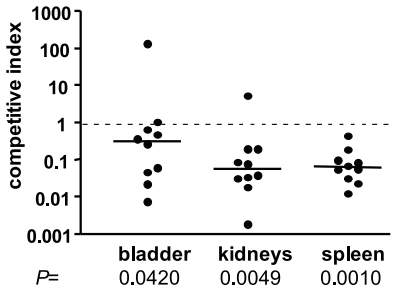

FIG. 7. HI4320 *gdhA*Ω*kan* is less fit *in vivo* than wild-type HI4320. Ten female CBA/J mice were transurethrally infected with a 1:1 mixture of HI4320 and HI4320 *gdhA*Ω*kan*. After 7 days, bacteria were enumerated in the bladder, kidneys, and spleen. The competitive index (CI) of the *gdhA* mutant compared to the wild type was plotted; each dot represents the CI from one mouse. The mutant was significantly outcompeted by the wild type in all three organs. Bars indicate median values.

There were several differences between *P. mirabilis* and *E. coli* transcription *in vivo*. Although both *P. mirabilis* and UPEC upregulate pyruvate catabolism pathways *in vivo*, there are more, and more highly upregulated, genes leading to acetate secretion by *P. mirabilis*. Increased acetate secretion, which lowers pH, might be a useful counter to urease-induced alkalinization. In addition to peptide uptake, surprisingly, *P. mirabilis* also upregulates genes involved in glucose uptake (*crr* and *ptsG*) and glycolysis (*pgi*, *pfkA*, and *gpmAB*) *in vivo*. Certainly, both *E. coli* and *P. mirabilis* can utilize glucose. With the exception of uncontrolled diabetes, generally glucose is not present in urine. Thus, the apparent ability of *P. mirabilis* to obtain glucose during UTI warrants further investigation.

With respect to nitrogen assimilation, there are some in-

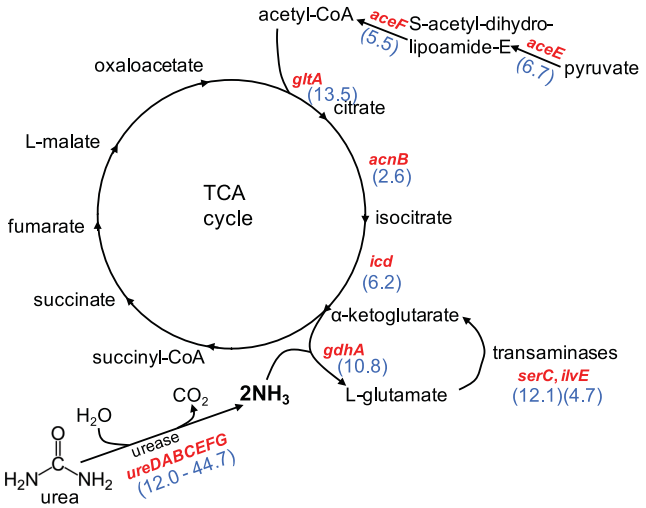

FIG. 8. *In vivo* upregulated genes suggest carbon-nitrogen balance drives *P. mirabilis* central metabolism. The intersection of the TCA cycle with pyruvate catabolism and ammonia assimilation is depicted. Genes upregulated *in vivo* >2-fold are shown in red; fold increases (blue) are indicated in parentheses.

triguing differences between *P. mirabilis* and UPEC transcription *in vivo*. The potent urease encoded by *P. mirabilis*, but absent in UPEC, ensures an abundant source of ammonia in the urinary tract (Fig. 8). Thus, while UPEC is starved for nitrogen *in vivo* (22, 74), the carbon-nitrogen balance for *P. mirabilis* may be flipped. Likewise, the genes encoding a portion of the TCA cycle (*gltA*, *acnB*, and *icd*), comprising the steps from acetyl coenzyme A (acetyl-CoA) formation to α-ketoglutarate synthesis, are upregulated by *P. mirabilis in vivo* (Fig. 8), while the rest of the TCA cycle genes in *P. mirabilis* were not differentially regulated *in vivo*. No such upregulation occurs in UPEC during UTI. (Indeed one gene, *acnA*, is even downregulated *in vivo*.) At this point in the *P. mirabilis* cycle, α-ketoglutarate can continue in the TCA cycle to make succinyl-CoA or be converted by incorporation of ammonia to generate L-glutamate via glutamate dehydrogenase (GDH). We initially hypothesized that expression of *gdhA* and *glnA* differs in *P. mirabilis* and UPEC in the urinary tract because of nitrogen availability.

Indeed, regulation of nitrogen uptake and assimilation is complex, with multiple levels of transcriptional and posttranslational control (reviewed in references 37 and 67). The carbon/nitrogen ratios for *P. mirabilis* and UPEC in the urinary tract are certainly not the same. Continuous high levels of GDH activity *in vivo* would lead to diminished α-ketoglutarate pools (30), and therefore, upregulation of upstream TCA cycle enzymes would be required to maintain the full TCA cycle (i.e., to convert α-ketoglutarate to succinyl-CoA) (Fig. 8). Although inverse *in vivo* regulation of *gdhA* and *glnA* by *P. mirabilis* and UPEC initially was suspected to be solely due to urease activity in *P. mirabilis*, this was not the case. Addition of exogenous ammonium (NH_4Cl) or intracellular ammonia (catalyzed by urease-mediated urea hydrolysis) in culture did not lead to the differential gene expression observed *in vivo*. However, choice of carbon source, such as citrate, a major component of urine, had a profound effect on *gdhA* expression. Rich media (19), the presence of specific amino acids in minimal medium (68), or a greater carbon/nitrogen ratio (69) have been reported to repress *gdhA*. Only when citrate was used as the carbon source, which forces the TCA cycle to operate, did we see a concomitant decrease in *glnA* expression. However, although *P. mirabilis* HI4320 can utilize citrate as a carbon source and *E. coli* cannot, there are more favorable carbon sources available in the urinary tract. Additionally, not all *P. mirabilis* strains utilize citrate as the sole carbon source (29), and future studies on such strains will be informative.

Glutamate dehydrogenase plays a critical metabolic role during *P. mirabilis* UTI. *gdhA* mutants, however, generally have only a subtle phenotype, if any, in other species (68). For example, an *E. coli gdhA* mutant only showed a defect when placed in direct competition with the wild-type parent strain in batch culture during glucose limitation (25). *Neisseria meningitidis* has also been shown to require *gdhA* for full virulence in an infant rat model (76), although this species lacks glutamate synthase (*gltBD*) (62, 78) and therefore cannot synthesize glutamate via the glutamine synthetase-GOGAT system (67). Furthermore, one of two *N. meningitidis gdhA* transcripts is regulated by adjoining gene *gdhR* (61), which is not found in enteric bacteria.

Global analysis of pathogens within the host continues to yield new insights into pathogenesis and central metabolism. This analysis of transcription during UTI will provide a baseline for future studies of early events in transcription, proteomics, tissue-specific expression, and mixed-species infections.

ACKNOWLEDGMENTS

This work was supported in part by Public Health Service grants AI043363 and AI059722 from the National Institutes of Health. M.M.P. was supported in part by National Research Service Award F32 AI068324.

We gratefully acknowledge critical discussions with Robert Bender, Christopher Alteri, and Patrick Vigil.

REFERENCES

1. **Alamuri, P., et al.** 2010. Adhesion, invasion, and agglutination mediated by two trimeric autotransporters in the human uropathogen *Proteus mirabilis*. Infect. Immun. **78:**4882–4894.
2. **Alamuri, P., and H. L. Mobley.** 2008. A novel autotransporter of uropathogenic *Proteus mirabilis* is both a cytotoxin and an agglutinin. Mol. Microbiol. **68:**997–1017.
3. **Allison, C., N. Coleman, P. L. Jones, and C. Hughes.** 1992. Ability of *Proteus mirabilis* to invade human urothelial cells is coupled to motility and swarming differentiation. Infect. Immun. **60:**4740–4746.
4. **Alteri, C. J., S. N. Smith, and H. L. Mobley.** 2009. Fitness of *Escherichia coli* during urinary tract infection requires gluconeogenesis and the TCA cycle. PLoS Pathog. **5:**e1000448.
5. **Altman, P. L.** 1961. Physical properties and chemical composition of urine: mammals. Part 1. Man, p. 363–369. *In* D. L. Dittmer (ed.), Blood and other bodily fluids. Federation of American Societies for Experimental Biology, Washington, DC.
6. **Aryee, M. J., J. A. Gutierrez-Pabello, I. Kramnik, T. Maiti, and J. Quackenbush.** 2009. An improved empirical Bayes approach to estimating differential gene expression in microarray time-course data: BETR (Bayesian Estimation of Temporal Regulation). BMC Bioinformatics **10:**409.
7. **Asscher, A. W., M. Sussman, W. E. Waters, R. H. Davis, and S. Chick.** 1966. Urine as a medium for bacterial growth. Lancet **ii:**1037–1041.
8. **Bahrani, F. K., et al.** 1994. Construction of an MR/P fimbrial mutant of *Proteus mirabilis*: role in virulence in a mouse model of ascending urinary tract infection. Infect. Immun. **62:**3363–3371.
9. **Bahrani, F. K., and H. L. Mobley.** 1993. *Proteus mirabilis* MR/P fimbriae: molecular cloning, expression, and nucleotide sequence of the major fimbrial subunit gene. J. Bacteriol. **175:**457–464.
10. **Belas, R., D. Erskine, and D. Flaherty.** 1991. Transposon mutagenesis in *Proteus mirabilis*. J. Bacteriol. **173:**6289–6293.
11. **Bijlsma, I. G., L. van Dijk, J. G. Kusters, and W. Gaastra.** 1995. Nucleotide

sequences of two fimbrial major subunit genes, *pmpA* and *ucaA*, from canine-uropathogenic *Proteus mirabilis* strains. Microbiology **141:**1349–1357.
12. **Burall, L. S., et al.** 2004. *Proteus mirabilis* genes that contribute to pathogenesis of urinary tract infection: identification of 25 signature-tagged mutants attenuated at least 100-fold. Infect. Immun. **72:**2922–2938.
13. **Clemmer, K. M., and P. N. Rather.** 2008. The Lon protease regulates swarming motility and virulence gene expression in *Proteus mirabilis*. J. Med. Microbiol. **57:**931–937.
14. **Connell, I., et al.** 1996. Type 1 fimbrial expression enhances *Escherichia coli* virulence for the urinary tract. Proc. Natl. Acad. Sci. U. S. A. **93:**9827–9832.
15. **Cook, S. W., N. Mody, J. Valle, and R. Hull.** 1995. Molecular cloning of *Proteus mirabilis* uroepithelial cell adherence (*uca*) genes. Infect. Immun. **63:**2082–2086.
16. **Dumanski, A. J., H. Hedelin, A. Edin-Liljegren, D. Beauchemin, and R. J. McLean.** 1994. Unique ability of the *Proteus mirabilis* capsule to enhance mineral growth in infectious urinary calculi. Infect. Immun. **62:**2998–3003.
17. **Feuillet, V., et al.** 2006. Involvement of Toll-like receptor 5 in the recognition of flagellated bacteria. Proc. Natl. Acad. Sci. U. S. A. **103:**12487–12492.
18. **Flannery, E. L., L. Mody, and H. L. Mobley.** 2009. Identification of a modular pathogenicity island that is widespread among urease-producing uropathogens and shares features with a diverse group of mobile elements. Infect. Immun. **77:**4887–4894.
19. **Goss, T. J., B. K. Janes, and R. A. Bender.** 2002. Repression of glutamate dehydrogenase formation in *Klebsiella aerogenes* requires two binding sites for the nitrogen assimilation control protein, NAC. J. Bacteriol. **184:**6966–6975.
20. **Griffith, D. P., D. M. Musher, and C. Itin.** 1976. Urease. The primary cause of infection-induced urinary stones. Invest. Urol. **13:**346–350.
21. **Hackbarth, H., D. Buttner, and K. Gartner.** 1982. Intraspecies allometry: correlation between kidney weight and glomerular filtration rate vs. body weight. Am. J. Physiol. **242:**R303–R305.
22. **Hagan, E. C., A. L. Lloyd, D. A. Rasko, G. J. Faerber, and H. L. Mobley.** 2010. *Escherichia coli* global gene expression in urine from women with urinary tract infection. PLoS Pathog. **6:**e1001187.
23. **Hagberg, L., et al.** 1983. Ascending, unobstructed urinary tract infection in mice caused by pyelonephritogenic *Escherichia coli* of human origin. Infect. Immun. **40:**273–283.
24. **Hamilton-Miller, J. M., and R. A. Gargan.** 1979. Rapid screening for urease inhibitors. Invest. Urol. **16:**327–328.
25. **Helling, R. B.** 1994. Why does *Escherichia coli* have two primary pathways for synthesis of glutamate? J. Bacteriol. **176:**4664–4668.
26. **Himpsl, S. D., C. V. Lockatell, J. R. Hebel, D. E. Johnson, and H. L. Mobley.** 2008. Identification of virulence determinants in uropathogenic *Proteus mirabilis* using signature-tagged mutagenesis. J. Med. Microbiol. **57:**1068–1078.
27. **Himpsl, S. D., et al.** 2010. Proteobactin and a yersiniabactin-related siderophore mediate iron acquisition in *Proteus mirabilis*. Mol. Microbiol. **78:**138–157.
28. **Hooton, T. M., et al.** 2010. Diagnosis, prevention, and treatment of catheter-associated urinary tract infection in adults: 2009 International Clinical Practice Guidelines from the Infectious Diseases Society of America. Clin. Infect. Dis. **50:**625–663.
29. **Janda, J. M., and S. L. Abbott.** 2006. The enterobacteria, 2nd ed. ASM Press, Washington, DC.
30. **Janes, B. K., et al.** 2001. Growth inhibition caused by overexpression of the structural gene for glutamate dehydrogenase (*gdhA*) from *Klebsiella aerogenes*. J. Bacteriol. **183:**2709–2714.
31. **Jansen, A. M., C. V. Lockatell, D. E. Johnson, and H. L. Mobley.** 2003. Visualization of *Proteus mirabilis* morphotypes in the urinary tract: the elongated swarmer cell is rarely observed in ascending urinary tract infection. Infect. Immun. **71:**3607–3613.
32. **Johnson, D. E., et al.** 1993. Contribution of *Proteus mirabilis* urease to persistence, urolithiasis, and acute pyelonephritis in a mouse model of ascending urinary tract infection. Infect. Immun. **61:**2748–2754.
33. **Jones, B. D., C. V. Lockatell, D. E. Johnson, J. W. Warren, and H. L. Mobley.** 1990. Construction of a urease-negative mutant of *Proteus mirabilis*: analysis of virulence in a mouse model of ascending urinary tract infection. Infect. Immun. **58:**1120–1123.
34. **Klevens, R. M., et al.** 2007. Estimating health care-associated infections and deaths in U.S. hospitals, 2002. Public Health Rep. **122:**160–166.
35. **Lane, M. C., C. J. Alteri, S. N. Smith, and H. L. Mobley.** 2007. Expression of flagella is coincident with uropathogenic *Escherichia coli* ascension to the upper urinary tract. Proc. Natl. Acad. Sci. U. S. A. **104:**16669–16674.
36. **Lane, M. C., X. Li, M. M. Pearson, A. N. Simms, and H. L. Mobley.** 2009. Oxygen-limiting conditions enrich for fimbriate cells of uropathogenic *Proteus mirabilis* and *Escherichia coli*. J. Bacteriol. **191:**1382–1392.
37. **Leigh, J. A., and J. A. Dodsworth.** 2007. Nitrogen regulation in bacteria and archaea. Annu. Rev. Microbiol. **61:**349–377.
38. **Li, X., et al.** 2004. Use of translational fusion of the MrpH fimbrial adhesin-binding domain with the cholera toxin A2 domain, coexpressed with the cholera toxin B subunit, as an intranasal vaccine to prevent experimental urinary tract infection by *Proteus mirabilis*. Infect. Immun. **72:**7306–7310.
39. **Li, X., et al.** 2004. Development of an intranasal vaccine to prevent urinary tract infection by *Proteus mirabilis*. Infect. Immun. **72:**66–75.
40. **Li, X., D. A. Rasko, C. V. Lockatell, D. E. Johnson, and H. L. Mobley.** 2001. Repression of bacterial motility by a novel fimbrial gene product. EMBO J. **20:**4854–4862.
41. **Li, X., et al.** 2002. Visualization of *Proteus mirabilis* within the matrix of urease-induced bladder stones during experimental urinary tract infection. Infect. Immun. **70:**389–394.
42. **Lima, A., P. Zunino, B. D'Alessandro, and C. Piccini.** 2007. An iron-regulated outer-membrane protein of *Proteus mirabilis* is a haem receptor that plays an important role in urinary tract infection and in *in vivo* growth. J. Med. Microbiol. **56:**1600–1607.
43. **Livak, K. J., and T. D. Schmittgen.** 2001. Analysis of relative gene expression data using real-time quantitative PCR and the $2^{-\Delta\Delta CT}$ method. Methods **25:**402–408.
44. **Loomes, L. M., B. W. Senior, and M. A. Kerr.** 1990. A proteolytic enzyme secreted by *Proteus mirabilis* degrades immunoglobulins of the immunoglobulin A1 (IgA1), IgA2, and IgG isotypes. Infect. Immun. **58:**1979–1985.
45. **Lucht, J. M., and E. Bremer.** 1994. Adaptation of *Escherichia coli* to high osmolarity environments: osmoregulation of the high-affinity glycine betaine transport system *proU*. FEMS Microbiol. Rev. **14:**3–20.
46. **Martinez, J. J., M. A. Mulvey, J. D. Schilling, J. S. Pinkner, and S. J. Hultgren.** 2000. Type 1 pilus-mediated bacterial invasion of bladder epithelial cells. EMBO J. **19:**2803–2812.
47. **Massad, G., F. K. Bahrani, and H. L. Mobley.** 1994. *Proteus mirabilis* fimbriae: identification, isolation, and characterization of a new ambient-temperature fimbria. Infect. Immun. **62:**1989–1994.
48. **Massad, G., J. F. Fulkerson, Jr., D. C. Watson, and H. L. Mobley.** 1996. *Proteus mirabilis* ambient-temperature fimbriae: cloning and nucleotide sequence of the *atf* gene cluster. Infect. Immun. **64:**4390–4395.
49. **Massad, G., C. V. Lockatell, D. E. Johnson, and H. L. Mobley.** 1994. *Proteus mirabilis* fimbriae: construction of an isogenic *pmfA* mutant and analysis of virulence in a CBA mouse model of ascending urinary tract infection. Infect. Immun. **62:**536–542.
50. **Massad, G., and H. L. Mobley.** 1994. Genetic organization and complete sequence of the *Proteus mirabilis pmf* fimbrial operon. Gene **150:**101–104.
51. **Mobley, H. L., et al.** 1996. Construction of a flagellum-negative mutant of *Proteus mirabilis*: effect on internalization by human renal epithelial cells and virulence in a mouse model of ascending urinary tract infection. Infect. Immun. **64:**5332–5340.
52. **Mobley, H. L., et al.** 1990. Pyelonephritogenic *Escherichia coli* and killing of cultured human renal proximal tubular epithelial cells: role of hemolysin in some strains. Infect. Immun. **58:**1281–1289.
53. **Mobley, H. L., and R. P. Hausinger.** 1989. Microbial ureases: significance, regulation, and molecular characterization. Microbiol. Rev. **53:**85–108.
54. **Mobley, H. L., and J. W. Warren.** 1987. Urease-positive bacteriuria and obstruction of long-term urinary catheters. J. Clin. Microbiol. **25:**2216–2217.
55. **Morgenstein, R. M., B. Szostek, and P. N. Rather.** 2010. Regulation of gene expression during swarmer cell differentiation in *Proteus mirabilis*. FEMS Microbiol. Rev. **34:**753–763.
56. **Mulvey, M. A., et al.** 1998. Induction and evasion of host defenses by type 1-piliated uropathogenic *Escherichia coli*. Science **282:**1494–1497.
57. **Nielubowicz, G. R., and H. L. Mobley.** 2010. Host-pathogen interactions in urinary tract infection. Nat. Rev. Urol. **7:**430–441.
58. **Nielubowicz, G. R., S. N. Smith, and H. L. Mobley.** 2008. Outer membrane antigens of the uropathogen *Proteus mirabilis* recognized by the humoral response during experimental murine urinary tract infection. Infect. Immun. **76:**4222–4231.
59. **Nielubowicz, G. R., S. N. Smith, and H. L. Mobley.** 2010. Zinc uptake contributes to motility and provides a competitive advantage to *Proteus mirabilis* during experimental urinary tract infection. Infect. Immun. **78:**2823–2833.
60. **Old, D. C., and R. A. Adegbola.** 1982. Haemagglutinins and fimbriae of *Morganella*, *Proteus* and *Providencia*. J. Med. Microbiol. **15:**551.
61. **Pagliarulo, C., et al.** 2004. Regulation and differential expression of *gdhA* encoding NADP-specific glutamate dehydrogenase in *Neisseria meningitidis* clinical isolates. Mol. Microbiol. **51:**1757–1772.
62. **Parkhill, J., et al.** 2000. Complete DNA sequence of a serogroup A strain of *Neisseria meningitidis* Z2491. Nature **404:**502–506.
63. **Pearson, M. M., and H. L. Mobley.** 2007. The type III secretion system of *Proteus mirabilis* HI4320 does not contribute to virulence in the mouse model of ascending urinary tract infection. J. Med. Microbiol. **56:**1277–1283.
64. **Pearson, M. M., D. A. Rasko, S. N. Smith, and H. L. Mobley.** 2010. Transcriptome of swarming *Proteus mirabilis*. Infect. Immun. **78:**2834–2845.
65. **Pearson, M. M., et al.** 2008. Complete genome sequence of uropathogenic *Proteus mirabilis*, a master of both adherence and motility. J. Bacteriol. **190:**4027–4037.
66. **Pellegrino, R., U. Galvalisi, P. Scavone, V. Sosa, and P. Zunino.** 2003. Evaluation of *Proteus mirabilis* structural fimbrial proteins as antigens against urinary tract infections. FEMS Immunol. Med. Microbiol. **36:**103–110.
67. **Reitzer, L.** 2003. Nitrogen assimilation and global regulation in *Escherichia coli*. Annu. Rev. Microbiol. **57:**155–176.

68. **Reitzer, L. J.** 1996. Ammonia assimilation and the biosynthesis of glutamine, glutamate, aspartate, asparagine, L-alanine, and D-alanine, p. 391–407. *In* F. C. Neidhardt et al. (ed.), *Escherichia coli* and *Salmonella typhimurium*: cellular and molecular biology, vol. 1. ASM Press, Washington, DC.
69. **Riba, L., B. Becerril, L. Servin-Gonzalez, F. Valle, and F. Bolivar.** 1988. Identification of a functional promoter for the Escherichia coli *gdhA* gene and its regulation. Gene **71:**233–246.
70. **Roos, V., and P. Klemm.** 2006. Global gene expression profiling of the asymptomatic bacteriuria *Escherichia coli* strain 83972 in the human urinary tract. Infect. Immun. **74:**3565–3575.
71. **Saeed, A. I., et al.** 2003. TM4: a free, open-source system for microarray data management and analysis. Biotechniques **34:**374–378.
72. **Sarada, K. V., N. A. Rao, and T. A. Venkitasubramanian.** 1980. Isolation and characterisation of glutamate dehydrogenase from *Mycobacterium smegmatis* CDC 46. Biochim. Biophys. Acta **615:**299–308.
73. **Scavone, P., V. Sosa, R. Pellegrino, U. Galvalisi, and P. Zunino.** 2004. Mucosal vaccination of mice with recombinant *Proteus mirabilis* structural fimbrial proteins. Microbes Infect. **6:**853–860.
74. **Snyder, J. A., et al.** 2004. Transcriptome of uropathogenic *Escherichia coli* during urinary tract infection. Infect. Immun. **72:**6373.
75. **Stadtman, E. R., P. Z. Smyrniotis, J. N. Davis, and M. E. Wittenberger.** 1979. Enzymic procedures for determining the average state of adenylylation of *Escherichia coli* glutamine synthetase. Anal. Biochem. **95:**275–285.
76. **Sun, Y. H., S. Bakshi, R. Chalmers, and C. M. Tang.** 2000. Functional genomics of *Neisseria meningitidis* pathogenesis. Nat. Med. **6:**1269–1273.
77. **Swihart, K. G., and R. A. Welch.** 1990. Cytotoxic activity of the *Proteus* hemolysin HpmA. Infect. Immun. **58:**1861–1869.
78. **Tettelin, H., et al.** 2000. Complete genome sequence of *Neisseria meningitidis* serogroup B strain MC58. Science **287:**1809.
79. **Tusher, V. G., R. Tibshirani, and G. Chu.** 2001. Significance analysis of microarrays applied to the ionizing radiation response. Proc. Natl. Acad. Sci.U. S. A. **98:**5116.
80. **Uphoff, T. S., and R. A. Welch.** 1990. Nucleotide sequencing of the *Proteus mirabilis* calcium-independent hemolysin genes (*hpmA* and *hpmB*) reveals sequence similarity with the *Serratia marcescens* hemolysin genes (*shlA* and *shlB*). J. Bacteriol. **172:**1206.
81. **Warren, J. W., et al.** 1987. Fever, bacteremia, and death as complications of bacteriuria in women with long-term urethral catheters. J. Infect. Dis. **155:** 1151–1158.
82. **Warren, J. W., J. H. Tenney, J. M. Hoopes, H. L. Muncie, and W. C. Anthony.** 1982. A prospective microbiologic study of bacteriuria in patients with chronic indwelling urethral catheters. J. Infect. Dis. **146:**719–723.
83. **Wassif, C., D. Cheek, and R. Belas.** 1995. Molecular analysis of a metalloprotease from *Proteus mirabilis*. J. Bacteriol. **177:**5790.
84. **Welch, R. A., et al.** 2002. Extensive mosaic structure revealed by the complete genome sequence of uropathogenic *Escherichia coli*. Proc. Natl. Acad. Sci. U. S. A. **99:**17020–17024.
85. **Wray, S. K., S. I. Hull, R. G. Cook, J. Barrish, and R. A. Hull.** 1986. Identification and characterization of a uroepithelial cell adhesin from a uropathogenic isolate of *Proteus mirabilis*. Infect. Immun. **54:**43–49.
86. **Zunino, P., et al.** 2003. *Proteus mirabilis* fimbriae (PMF) are important for both bladder and kidney colonization in mice. Microbiology **149:**3231–3237.
87. **Zunino, P., et al.** 2007. Mannose-resistant *Proteus*-like and *P. mirabilis* fimbriae have specific and additive roles in *P. mirabilis* urinary tract infections. FEMS Immunol. Med. Microbiol. **51:**125–133.

Editor: S. R. Blanke